Macromolecules
NOTE

Macromolecules **2009**, *42*, 7213–7216 **7213**
DOI: 10.1021/ma9011413

Fabrication of Nanoporous Block Copolymer Thin Films through Mediation of Interfacial Interactions with UV Cross-Linked Polystyrene

Wei Chen, Soojin Park,[†] Jia-Yu Wang,[‡] and Thomas P. Russell*

Department of Polymer Science & Engineering, University of Massachusetts, Amherst, Massachusetts 01003 [†]Current address: School of Energy Engineering, Ulsan National Institute of Science and Technology, Ulsan, 689-798 Korea. [‡]Current address: Department of Chemistry, The University of Chicago, Chicago, Illinois 60637

Received May 26, 2009; Revised Manuscript Received August 10, 2009

Introduction

Porosity control of inorganic and organic nanoporous materials is increasingly critical for applications ranging from filtration membranes to patterned templates and photonic materials. Recently, block copolymers (BCPs) have received much attention as templates and scaffolds for nanoporous materials that have potential use in optics and microelectronics due to their ability to form periodical nanostructures.[1−8] One of the most common strategies to generate nanopores in polymer thin films is selective UV degradation and removal of the minor-component microdomains.[8] Here, an orientation of BCP microdomains normal to the film surfaces is usually required. However, the preferential interaction of one block of the BCP with the substrate or a lower surface energy of one component, in general, results in the segregation of one block to either the underlying substrate or the surface. As a result of connectivity of the blocks, this preferential interaction causes the BCP microdomains to orient parallel to the substrate. Consequently, controlling the interfacial interactions is important for the optimal fabrication of nanoporous BCP thin films.[9]

Surface modification via polymer brushes attached to a substrate to manipulate interfacial interactions is a robust strategy to control the orientation of BCP microdomains in thin films.[10−19] In the case of polystyrene-*block*-poly(methyl methacrylate) (PS-*b*-PMMA) on a silicon substrate, mediated interfacial interactions can be achieved by anchoring random copolymers to the substrate where the composition of the random copolymer can be adjusted to control the interfacial interactions between PS and PMMA blocks.[20] Russell and coworkers demonstrated that the grafting of end-hydroxyl functionalized PS-*r*-PMMA copolymers having f_{st} (where f_{st} is the styrene fraction) of 0.58 yielded neutral conditions, which $\Delta\gamma = |\gamma_{PS,S} - \gamma_{PMMA,S}| = 0$, where $\gamma_{PS,S}$ and $\gamma_{PMMA,S}$ are the interfacial tensions between two blocks (PS and PMMA) and the substrate (S). A vertical orientation of lamellar or cylindrical domains could be achieved, as long as the thickness of the film is $\sim L_0$, the repeat period of the BCP, or less.[10,17] Although this surface modification had proven to be robust and easily applied to very large-area surfaces, this surface modification is restricted to homogeneous oxide surfaces. Sequently, Ryu et al. developed a method where the interfacial interactions of any surface could be manipulated using a thin film of cross-linkable benzocyclobutene (BCB)-functionalized random copolymers with styrene and methyl methacrylate, P(S-*r*-BCB-*r*-MMA).[11,13] This process can be used on any substrate, flexible or rigid, homogeneous or heterogeneous,[11] but a high temperature (> 200 °C) is required for efficient cross-linking. Hawker, Gopalan and co-workers[14−16] investigated several photo-cross-linkable random copolymers where alternative functional groups, such as acryloyl, glycidyl, and azido groups, could be selectively cross-linked by UV radiation. Recently, Nealey and co-workers[18,19] made neutral wetting brushes using a ternary blend of homopolymers A and B and a low-molecular-weight A-*b*-B BCP. The utility of all these random copolymers, though, may be limited by the functional monomers that are difficult to synthesize or are not commercially available. In addition, due to the low χ value of PS-*b*-PMMA,[21,22] the smallest attainable pore size is limited by the product of χN, where χ is the Flory−Huggins segmental interaction parameter and N is the number of segments in the BCP. Currently, only pore diameters ranging from 14 to 50 nm have been produced.[23]

Here, we fabricated nanoporous thin films of brominated polystyrene-*block*-poly(methyl methacrylate) (PBrS-*b*-PMMA) copolymers by using UV cross-linked PS matte for mediating preferential interfacial interactions to achieve the perpendicular orientation of the microdomains. In contrast to PS-*b*-PMMA copolymers, PBrS-*b*-PMMA copolymers are more strongly microphase-separated, so that pore diameters can be extended to 10 nm or less.

Experimental Section

Synthesis of PBrS-*b*-PMMA. PS-*b*-PMMA di-BCPs used in this work were synthesized by sequential living anionic polymerization. The number-average molecular weights (M_n) are 17.7, 28.2, and 98.5 kg/mol; the polydispersity indices (PDIs) are 1.06, 1.04, and 1.04, and the volume fractions of PS are 69.7%, 67.7%, and 67.4%, respectively. Molecular weights and PDIs were characterized by gel permeation chromatography (GPC), and the compositions of copolymers were determined by ^{1}H nuclear magnetic resonance (NMR) with mass densities of two components (1.05 and 1.18 g/cm^3 for PS and PMMA). Brominations of phenyl rings were carried out in a similar way reported previously[24,25] (see the Supporting Information for details).

Preparation of Thin Films. A 0.5 wt % solution of PS homopolymer (M_n = 13.3 kg/mol and PDI = 1.12) in toluene was spin-coated at 3000 rpm onto Si wafers, yielding ~13 nm thick films. The Si wafers were first cleaned by a procedure described elsewhere.[10,26] The thin films were cured by UV radiation with an intensity of ~5 mW/cm^2 under vacuum for 3 h. Subsequently, the films were thoroughly rinsed with toluene to remove un-cross-linked PS, and the thickness of insoluble cross-linked PS as measured by ellipsometry was 9 nm. The volume shrinkage observed can be attributed to the removal of un-cross-linked homopolymer, the volume reduction inherent to cross-linking, and small portion of PS degradation under UV exposure.[27] Reducing irradiation time led to a decrease in degree of cross-linking, since the film exposed for 1 h was easily removed with a good solvent;

*To whom correspondence should be addressed: e-mail russell@mail.pse.umass.edu.

Published on Web 08/24/2009

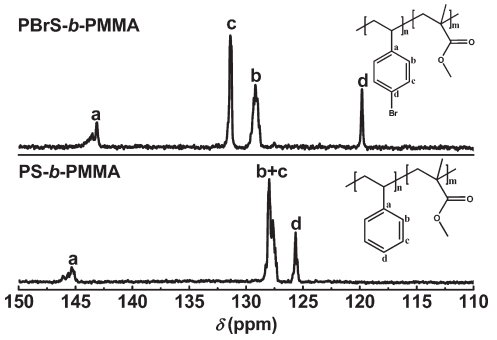

Figure 1. ^{13}C NMR spectra for PS-*b*-PMMA copolymer before (bottom) and after (top) bromination.

while for the film exposed for 2 h, the thickness gradually decreased by continued rinsing with a good solvent. PBrS-*b*-PMMA thin films with cylindrical morphology were prepared on the substrates with a cross-linked PS matte and then annealed for 24 h at 190 °C under vacuum to orient the cylindrical microdomains normal to the surface. Finally, the copolymer thin films were exposed to by UV radiation with an intensity of ~5 mW/cm^2 under vacuum for 35 min, followed by rinsing with acetic acid and deionized water. This cross-linked PBrS matrix and removed PMMA cylindrical microdomains, generating nanopores in the copolymer thin films. The pore diameters of nanoporous PBrS-*b*-PMMA thin films were determined by averaging the results from AFM and TEM image analyses.

Characterization. Small-angle X-ray scattering (SAXS) experiments were performed at Materials Research Science and Engineering Center (MRSEC) at the University of Massachusetts, Amherst. A SAXS instrument, consisting of a three-pinhole collimation system, had an Osmic MaxFlux X-ray (Cu Kα, 0.154 nm) source generated by a copper anode. SAXS measurements were performed at room temperature under vacuum with an exposure time of 60−120 min. All SAXS data presented here are raw data and not corrected for background and empty cell scattering. Grazing incidence small-angle X-ray scattering (GISAXS) measurements were performed at X22B beamline at National Synchrotron Light Source at Brookhaven National Laboratory using X-rays with a wavelength of $\lambda = 1.517$ Å with an exposure time of 60 s per frame. Typical GISAXS patterns were taken at an incidence angle of 0.20°, above the critical angles of the copolymer but below the critical angle of the silicon substrate. Consequently, the entire structure of copolymer thin films could be detected. Scanning force microscopy (SFM) images were obtained in both height and phase-contrast mode using a Digital Instruments (Dimension 3000) in the tapping mode. Fourier transform infrared (FT-IR) absorption spectra of the copolymer films were collected on a BioRad ExCalibur spectrometer with a resolution of 1 cm^{-1} over a wavenumber range from 4000 to 400 cm^{-1}. Spectra were obtained by using copolymer films cast on high resistance silicon wafers with a bare wafer providing the background spectrum. NMR spectra were recorded in $CDCl_3$ on Bruker Avance 400 (^1H) and 100 (^{13}C) MHz NMR spectrometer with a Bruker BBO5 probe. Molecular weights and PDIs were estimated by GPC in THF at 1.0 mL/min against linear polystyrene standards (Knauer pump K-501, refractive index detector K-2301, and three Polymer Laboratories Mixed D columns (5 μm, 300 mm × 7.5 mm)). TEM measurements were performed on a JEOL TEM200CX at an accelerating voltage of 200 kV.

Results and Discussion

PBrS-*b*-PMMA copolymers were prepared by bromination of PS-*b*-PMMA copolymers in nitrobenzene, a highly polar solvent, without catalyst. Shown in Figure 1 are ^{13}C NMR spectra of PS-*b*-PMMA copolymers, with a molecular weight

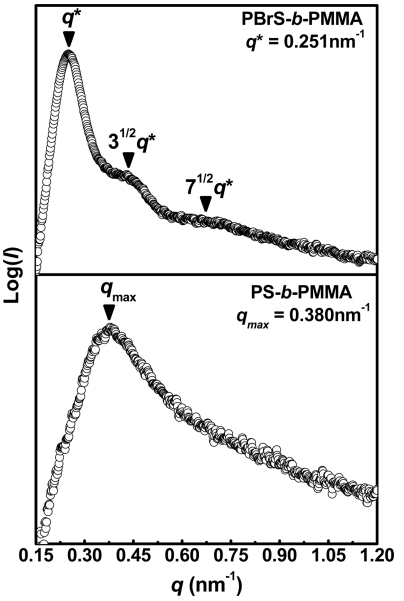

Figure 2. SAXS profiles for PS-*b*-PMMA copolymer with a molecular weight of 28.2 kg/mol (bottom) and the corresponding brominated copolymer (top). Both of them were thermally annealed at 190 °C for 24 h.

of 28.2 kg/mol, before and after bromination. After bromination, four peaks are seen at 120, 129, 131, and 143 ppm, in contrast to the original peaks at 126, 127−128, and 145 ppm for the PS-*b*-PMMA BCPs. These data confirmed that bromination occurred exclusively on benzene ring and only in the para position, in agreement with those early reports.[24,25] In addition, the peak at 126 ppm disappeared for the PBrS-*b*-PMMA copolymers, indicating that the styrene units were completely brominated. Both NMR and FT-IR spectra (Figure S1 and S2 in the Supporting Information) indicated that no obvious bromination of the backbone occurred. Since PS-*b*-PMMA copolymers are weakly segregated with a low χ value ($\chi = 0.0294 + 3.2/T$),[21,22] the low-molecular-weight PS-*b*-PMMA BCPs used in this study are in a phase-mixed, disordered state at room temperature. SAXS profile (log($I(q)$) vs $q = 4\pi \sin\theta/\lambda$, where q is the scattering vector, 2θ is the scattering angle, and $I(q)$ is the intensity) for the PS-*b*-PMMA copolymer with a molecular weight of 28.2 kg/mol showed a single, broad reflection with a peak centered near q_{max} of 0.380 nm^{-1}, arising from the correlation-hole scattering of a BCP in the disordered state (Figure 2). A very sharp peak at q^* of 0.251 nm^{-1} with two higher order reflection at $\sqrt{3}q^*$ and $\sqrt{7}q^*$ are seen in the SAXS profile of the corresponding PBrS-*b*-PMMA copolymer, demonstrating that a cylindrical microdomain morphology is well-developed and that the bromination has significantly enhanced the segmental interactions between the PBrS and PMMA blocks. Therefore, smaller microdomain sizes can be obtained for PBrS-*b*-PMMA copolymers.

It is well-known that interfacial interactions dictate the wetting layer at both polymer/substrate and polymer/air interfaces and, consequently, the orientation of microdomains in the films.[26,28−34] When $\Delta\gamma = |\gamma_{AS} - \gamma_{BS}| = 0$, where γ_{ij} is the interfacial tension between two components i and j, namely block A, block B, and the substrate (S), the interactions of the two blocks with the substrate are balanced, either equally attractive or repulsive. For films with a thickness of ~L_0, where L_0 is the natural period of the structures in bulk, the microdomains will align normal to the surface. However, for nonzero values of $\Delta\gamma$ close to zero and with the thickness not equal to L_0, stretching or compression of the copolymer can occur, and the relative values of the stretching and interfacial energies will dictate the perpendicular orientation

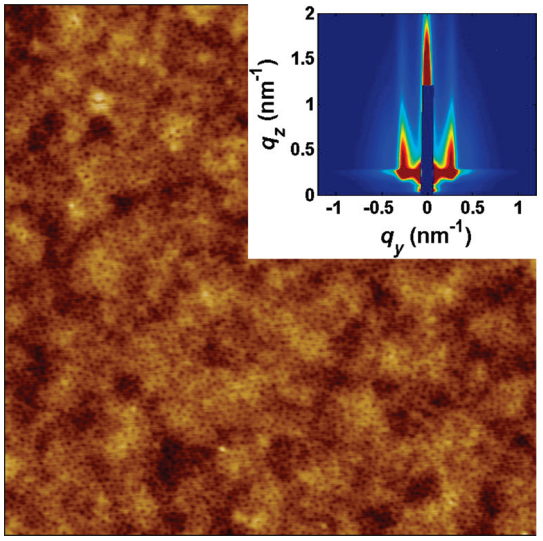

Figure 3. SFM height images (2 μm × 2 μm) of a thin film of PBrS-*b*-PMMA copolymer with a molecular weight of 28.2 kg/mol on the Si wafer coated with a layer of UV cross-linked PS homopolymer. The film was thermally annealed at 190 °C for 24 h, and then PMMA was selectively removed by exposing the film to UV radiation and rinsing with acetic acid to enhance contrast. The inset shows a representative GISAXS pattern of the nanoporous thin film.

of BCP microdomains.[10,12,26,35−39] The interfacial tension between PS and PMMA (~0.85 dyn/cm) is close to that between PS and PBrS (~1 dyn/cm).[40−44] Consequently, PS can meditate the interfacial interactions between BCPs and the substrate to orient the microdomains of PBrS-*b*-PMMA copolymers normal to the substrate in thin films, but the price of the two interfacial tensions that do not exactly match each other will have to be paid by the decrease of film thickness.

A ~10 nm thick film of the above PBrS-*b*-PMMA copolymers was spin-coated onto a Si substrate modified with the UV cross-linked PS matte. Following thermal annealing in vacuum at 190 °C for 24 h and removal of PMMA blocks by UV degradation and acetic acid rinsing, the resultant nanoporous thin film was examined by SFM and GISAXS (Figure 3). Nanopores, with diameters of ~10 nm, were seen in the PBrS matrix in both height and phase images. A more detailed description of the pore structure was obtained by GISAXS. In the scattering geometry, q_y is the scattering vector normal to the incidence plane (i.e., in the plane of the film), and the domain spacing is related to q_y by $d = 2\pi/q_y$. The incidence angle was at 0.20°, which is above the critical angle of the BCP film (~0.17°) but below the critical angle of the silicon substrate (~0.23°). Consequently, the X-rays penetrate into the entire film and probe the internal structures of the thin film. In the inset of Figure 3, the GISAXS pattern shows a sharp first-order scattering at ~25 nm (consistent with that seen in the bulk) with a second-order peak located a scattering vector ratio of 1:$\sqrt{3}$, corresponding to the first- and second-order reflection of the cylindrical pores oriented normal to the film surface. The absence of reflections along q_z (normal to the film surface) and the extension of the scattering along q_z are consistent with a structure of cylindrical pores oriented normal to the film surface that penetrate through the entire film.

The effectiveness of the UV cross-linked PS matte in mediating interfacial interactions was further examined with an asymmetric PBrS-*b*-PMMA copolymers having a higher molecular weight of 98.5 kg/mol. SFM images showed hexagonal PMMA microdomains oriented normal to the film surface with a center-to-center distance of 53.5 nm (Figure S3), consistent with GISAXS observations of two scattering rods with a ratio of peak positions of 1:$\sqrt{3}$ along the q_y. As for the lower-molecular-weight

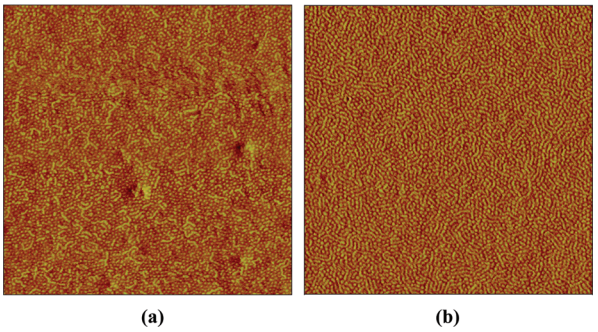

Figure 4. SFM phase images (2 μm × 2 μm) of PBrS-*b*-PMMA copolymer thin films with the thickness of ~12 nm and ~18 nm on the Si wafer coated with a layer of UV cross-linked PS homopolymer. The film was thermally annealed at 190 °C for 24 h.

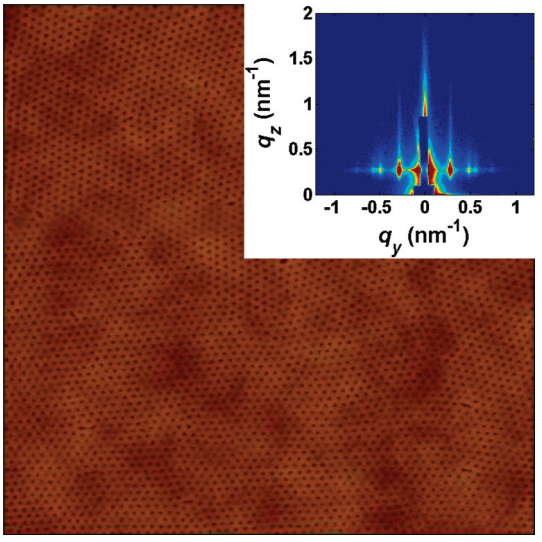

Figure 5. SFM height image (2 μm × 2 μm) a thin film of PBrS-*b*-PMMA copolymer with a molecular weight of 28.2 kg/mol on Si wafer coated with a layer of UV cross-linked PS homopolymer. The film was solvent-annealed in the toluene/THF (70/30, v/v) mixed vapors for 2 h, and then PMMA was selectively removed by exposing the film to UV radiation and rinsing with acetic acid to enhance contrast. The inset is a representative GISAXS pattern of the nanoporous thin film.

PS-*b*-PMMA copolymer, a nanoporous thin film with a pore diameters of 8 nm could be successfully obtained (Figure S4). However, the lateral ordering of nanopores was poor due to the small value of χN.[45]

Although UV cross-linked PS matte can effectively mediate interfacial interactions, the mismatch of interfacial energies as mentioned above have to be compensated by stretching copolymer chains via a decrease in the film thickness, significantly narrowing the thickness window for the cylindrical microdomain orientation normal to the substrate which differs from PS-*b*-PMMA.[10,12,26,46] Consequently, a perpendicular orientation of the PBrS-*b*-PMMA microdomains was only obtained in the films with thicknesses of ~10 nm, less than half of the intercylinder spacing. As shown in Figure 4, the increased film thickness reduced the stretching of the copolymer chains, causing the orientation of the microdomains to change for thicker films. The wormlike cylinders oriented parallel to the films surface were observed in the film with a thickness of ~12 nm and as the film thickness was increased to ~18 nm. Solvent annealing is another strategy to control the orientation of BCP microdomains, even having a higher lateral ordering.[2,8,47] However, one of its drawbacks is that there usually exists a very thin wetting layer of one block of the copolymers between the film and the substrate due to

preferential interfacial interactions. Combining two above-mentioned methods together, both of their drawbacks can be overcome, removing the wetting layer and increasing film thickness. A ~25 nm nanoporous PBrS-*b*-PMMA thin film was obtained after annealing under a toluene/THF mixed vapor (70/30, v/v) in small closed vessel for 2 h. SFM image showed vertical nanopores in a PBrS matrix having a higher degree of lateral ordering (Figure 5). A series of Bragg rods at relative peak positions of $1:\sqrt{3}:\sqrt{4}:\sqrt{7}$ along the q_y in the GISAXS pattern further confirmed that the highly ordered perpendicular nanopores were produced.

In summary, we have shown that a UV cross-linked PS matte can mediate the interfacial interaction for PBrS-*b*-PMMA copolymers, over a broad range of molecular weights having cylindrical microdomain morphology. Because of the enhanced χ between PBrS and PMMA blocks, cylindrical microdomains with diameters as small as ~8 nm could be obtained. Combining mediation of interfacial interactions and solvent annealing produced the nanoporous PBrS-*b*-PMMA thin film with perpendicular orientation and a high degree of lateral ordering. In addition, a particularly attractive feature of PBrS-*b*-PMMA copolymers is that active Br atoms provide an easy way to functionalize PBrS-*b*-PMMA copolymer thin films through palladium-catalyzed coupling reactions.

Acknowledgment. This work was supported by the U.S. Department of Energy Basic Energy Science. We thank B. Ocko and T. Hoffmann at Brookhaven National Laboratory for the assistance with GISAXS experiments. The use of the National Synchrotron Light Source (Contract DE-AC02-98CH10886) was supported by U.S. Department of Energy, Office of Science, Office of Basic Energy Sciences.

Supporting Information Available: Synthetic procedure, NMR and FT-IR data, additional SFM images and GISAXS patterns, pore size determination. This material is available free of charge via the Internet at http://pubs.acs.org.

References and Notes

(1) Ross, C. A.; Cheng, J. Y. *MRS Bull.* **2008**, *33*, 838–845.
(2) Hawker, C. J.; Russell, T. P. *MRS Bull.* **2005**, *30*, 952–966.
(3) Segalman, R. A. *Mater. Sci. Eng.* **2005**, *R48*, 191–226.
(4) Li, M.; Coenjarts, C. A.; Ober, C. K. *Adv. Polym. Sci.* **2005**, *190*, 183–226.
(5) Park, C.; Yoon, J.; Thomas, E. L. *Polymer* **2003**, *44*, 6725–6760.
(6) Li, M.; Ober, C. K. *Mater. Today* **2006**, *9*, 30–39.
(7) Stoykovich, M. P.; Nealey, P. F. *Mater. Today* **2006**, *9*, 20–29.
(8) Wang, J.-Y.; Chen, W.; Russell, T. P. Patterning with block polymers. In *Unconventional Nanopatterning Techniques and Applications*; Rogers, J. A., Lee, H. H., Eds.; John Wiley & Sons: Hoboken, NJ, 2009; pp 233−289.
(9) Fasolka, M. J.; Mayes, A. M. *Annu. Rev. Mater. Res.* **2001**, *31*, 323–355.
(10) Mansky, P.; Liu, Y.; Huang, E.; Russell, T. P.; Hawker, C. *Science* **1997**, *275*, 1458–1460.
(11) Ryu, D. Y.; Shin, K.; Drockenmuller, E.; Hawker, C. J.; Russell, T. P. *Science* **2005**, *308*, 236–239.
(12) Huang, E.; Russell, T. P.; Harrison, C.; Chaikin, P. M.; Register, R. A.; Hawker, C. J.; Mays, J. *Macromolecules* **1998**, *31*, 7641–7650.
(13) Ryu, D. Y.; Wang, J.-Y.; Lavery, K. A.; Drockenmuller, E.; Satija, S. K.; Hawker, C. J.; Russell, T. P. *Macromolecules* **2007**, *40*, 4296–4300.
(14) Bang, J.; Bae, J.; Löwenhielm, P.; Spiessberger, C.; Given-Beck, S. A.; Russell, T. P.; Hawker, C. J. *Adv. Mater.* **2007**, *19*, 4552–4557.
(15) Han, E.; In, I.; Park, S.-M.; La, Y.-H.; Wang, Y.; Nealey, P. F.; Gopalan, P. *Adv. Mater.* **2007**, *19*, 4448–4452.
(16) Han, E.; Stuen, K. O.; Leolukman, M.; Liu, C.-C.; Nealey, P. F.; Gopalan, P. *Macromolecules* **2009**, *42*, 4896–4901.
(17) Ham, S.; Shin, C.; Kim, E.; Ryu, D. Y.; Jeong, U.; Russell, T. P.; Hawker, C. J. *Macromolecules* **2008**, *41*, 6431–6437.
(18) Ji, S.; Liu, G.; Zheng, F.; Craig, G. S. W.; Himpsel, F. J.; Nealey, P. F. *Adv. Mater.* **2008**, *20*, 3054–3060.
(19) Ji, S.; Liu, C.-C.; Son, J. G.; Gotrik, K.; Craig, G. S. W.; Gopalan, P.; Himpsel, F. J.; Char, K.; Nealey, P. F. *Macromolecules* **2008**, *41*, 9098–9103.
(20) Kellogg, G. J.; Walton, D. G.; Mayes, A. M.; Lambooy, P.; Russell, T. P.; Gallagher, P. D.; Satija, S. K. *Phys. Rev. Lett.* **1996**, *76*, 2503–2506.
(21) Russell, T. P.; Hjelm, R. P. Jr.; Seeger, P. A. *Macromolecules* **1990**, *23*, 890–893.
(22) Wang, J.-Y.; Chen, W.; Russell, T. P. *Macromolecules* **2008**, *41*, 4904–4907.
(23) Xu, T.; Kim, H.-C.; DeRouchey, J.; Seney, C.; Levesque, C.; Martin, P.; Stafford, C. M.; Russell, T. P. *Polymer* **2001**, *42*, 9091–9095.
(24) Kambour, R. P.; Bendler, J. T.; Bopp, R. C. *Macromolecules* **1983**, *16*, 753–757.
(25) Kambour, R. P.; Bendler, J. T. *Macromolecules* **1986**, *19*, 2679–2682.
(26) Mansky, P.; Russell, T. P.; Hawker, C. J.; Mays, J.; Cook, D. C.; Satija, S. K. *Phys. Rev. Lett.* **1997**, *79*, 237–240.
(27) Chada, S.; Yan, M. *Soft Matter* **2008**, *4*, 2164–2167.
(28) Menelle, A.; Russell, T. P.; Anastasiadis, S. H.; Satija, S. K.; Majkrzak, C. F. *Phys. Rev. Lett.* **1992**, *68*, 67–70.
(29) Bassereau, P.; Brodbreck, D.; Russell, T. P.; Brown, H. R.; Shull, K. R. *Phys. Rev. Lett.* **1993**, *71*, 1716–1719.
(30) Factor, B. J.; Russell, T. P.; Toney, M. F. *Phys. Rev. Lett.* **1991**, *66*, 181–1184.
(31) Russell, T. P.; Menelle, A.; Anastasiadis, S. H.; Satija, S. K.; Majkrzak, C. F. *Prog. Colloid Polym. Sci.* **1993**, *91*, 97–100.
(32) Russell, T. P.; Menelle, A.; Anastasiadis, S. H.; Satija, S. K.; Majkrzak, C. F. *Phys. Rev. Lett.* **1993**, *70*, 1352.
(33) Green, P. F.; Christensen, T. M.; Russell, T. P.; Jerome, R. *J. Chem. Phys.* **1990**, *92*, 1478–1482.
(34) Rockford, L.; Liu, Y.; Mansky, P.; Russell, T. P.; Yoon, M.; Mochrie, S. G. J. *Phys. Rev. Lett.* **1999**, *82*, 2602–2605.
(35) Huang, E.; Rockford, L.; Russell, T. P.; Hawker, C. J. *Nature* **1998**, *395*, 757–758.
(36) Pickett, G. T.; Witten, T. A.; Nagel, S. R. *Macromolecules* **1993**, *26*, 3194–3199.
(37) Turner, M. S.; Johner, A.; Joanny, J. F. *J. Phys. I* **1995**, *5*, 917–932.
(38) Turner, M. S.; Joanny, J.-F. *Macromolecules* **1992**, *25*, 6681–6689.
(39) Tsori, Y.; Sivaniah, E.; Andelman, D.; Hashimoto, T. *Macromolecules* **2005**, *38*, 7193–7196.
(40) Zhang, X.; Kim, J. K. *Macromol. Rapid Commun.* **1998**, *19*, 499–504.
(41) Walton, D. G.; Kellogg, G. J.; Mayes, A. M.; Lambooy, P.; Russell, T. P. *Macromolecules* **1994**, *27*, 6225–6228.
(42) Slep, D.; Asselta, J.; Rafailovich, M. H.; Sokolov, J.; Winesett, D. A.; Smith, A. P.; Ade, H.; Anders, S. *Langmuir* **2000**, *16*, 2369–2375.
(43) Gorga, R. E.; Jablonski, E. L.; Thiyagarajan, P.; Seifert, S.; Balaji, N. *J. Polym. Sci., Polym. Phys.* **2002**, *40*, 255–271.
(44) Zhao, W.; Zhao, X.; Rafailovich, M. H.; Sokolov, J.; Mansfield, T.; Stein, R. S.; Composto, R. C.; Kramer, E. J.; Jones, R. A. L.; Sansone, M.; Nelson, M. *Physica B: Condens. Matter* **1991**, *173*, 43–46.
(45) Wang, J.-Y.; Leiston-Belanger, J. M.; Sievert, J. D.; Russell, T. P. *Macromolecules* **2006**, *39*, 8487–8491.
(46) Ryu, D. Y.; Ham, S.; Kim, E.; Jeong, U.; Hawker, C. J.; Russell, T. P. *Macromolecules* **2009**, *42*, 4902–4906.
(47) Kim, S. H.; Misner, M. J.; Russell, T. P. *Adv. Mater.* **2008**, *20*, 4851–4856.